



ELSEVIER

Contents lists available at ScienceDirect

Digital Applications in Archaeology and Cultural Heritage

journal homepage: www.elsevier.com/locate/daach

Recent improvements in photometric stereo for rock art 3D imaging

R. Dessì^a, C. Mannu^a, G. Rodriguez^{b,*}, G. Tanda^c, M. Vanzi^a^a Department of Electrical and Electronic Engineering, University of Cagliari, Piazza d'Armi 1, 09123 Cagliari, Italy^b Department of Mathematics and Computer Science, University of Cagliari, viale Merello 92, 09123 Cagliari, Italy^c Department of Archaeological and Historical-Artistic Sciences, University of Cagliari, Piazza Arsenale 1, 09124 Cagliari, Italy

ARTICLE INFO

Article history:

Received 30 September 2014

Received in revised form

15 May 2015

Accepted 19 May 2015

Available online 2 June 2015

Keywords:

Photometric stereo

Shape from shading

Domus de Janas

Sardinia neolithic tombs

ABSTRACT

Recent improvements in photometric stereo (PS) are shown to remove the major limitations of this low-cost 3D recording technique. In particular, there are significant improvements in lighting constraints, processing time and presence of deformation in reconstructed surfaces, allowing for fast and accurate restoration of shape and color information. The shooting technique is sufficiently easy to make PS ideal for ancient rock art, which is generally encountered in difficult to access sites, where many of the rock engravings to survey are often placed in a narrow space. This paper focuses on the Sardinia neolithic tombs known as Domus de Janas, as they offer an opportunity to demonstrate the applicability of PS to general rock art.

© 2015 Elsevier Ltd. All rights reserved.

1. Introduction

The role of 3D techniques in rock art documentation is crucial for several reasons. On one hand, the findings are frequently located in difficult to access positions and current protocols exclude any physical contact for creating replicas. On the other hand, the nature of rock art itself calls for 3D reconstruction: the handicrafts are small volume details engraved or sculptured out of wide natural surfaces, often corroded by millenary exposition to weather agents and coated with patinas.

Ordinary photography often requires several shots under different light conditions, in order to reveal all the details of a decorated surface. A contact-less accurate 3D recording is then an ideal solution: virtual reconstruction of the sole shape allows for removal of surface texture and for interactively applying virtual lights, even from directions impossible on site because of existing obstructions.

The difficulty to access many sites and the number of items to be documented, often as large as several thousand in the same site, makes many popular 3D-recording techniques impractical. Laser scanning hardly applies, because it requires a long acquisition time, not to mention the large cost of the instrumentation.

In this paper we go back to a technique as old as photometric stereo (PS) (Woodham, 1980). It is a photographic method that uses a fixed camera and a movable light to acquire a set of images that are proven to embed shape and color (albedo) information of

the framed object (Christensen and Shapiro, 1994). The principles are clearly described in the quoted seminal paper, but practical PS never achieved large popularity because of severe limitations. The ideal PS requires some lights oriented along known directions, with uniform intensity and low divergence (Barsky and Petrou, 2003). Any deviation from these constraints results in a poor reconstruction, often affected by distortion, and in an incomplete separation of the shape from the albedo.

A theoretical significant improvement has been achieved in 2006 (Chen and Chen, 2006); see also Basri and Jacobs (2007) which proposes a different approach based on the decomposition of the light intensity, as a function of direction, into linear combinations of spherical harmonics. The target of these new methods is to release the need for accurate location of the light directions, aiming at obtaining this information from the available set of images. This opens the possibility of freehand lighting, removing the requirement for accurate positioning of lamps, one of the most difficult issues in practical PS.

Despite this improvement, other intrinsic limitations typical of PS remain, e.g., the distortion for the steepest parts of the recorded object and the presence of casted shadows, which introduce blind regions in the reconstructed surface. A reduction of the computational complexity is also crucial: a processing time excessively long may lead to the impossibility of processing data during field acquisition, with the result that any shooting mistakes are revealed possibly hours later, when the site has been abandoned.

Another important limitation is the general assumption that the object surface is Lambertian; see Eq. (3.1) in Section 3. No real object satisfies exactly this hypothesis, and the presence of a small specular component in the reflectivity of the surface material can distort the direction of the normal vectors. This is a problem

* Corresponding author.

E-mail addresses: richidessi@gmail.com (R. Dessì), ca.mannu@gmail.com (C. Mannu), rodriguez@unica.it (G. Rodriguez), gtanda@unica.it (G. Tanda), vanzid@diee.unica.it (M. Vanzi).

typical in the use of PS, which cannot be easily removed, but during our field experience it did not cause an evident distortion in the reconstructions, at least in rock art documentation; see the images in Section 5. We believe that one of the keys to this self-correction is the redundancy of information used by our algorithm, that is, the fact that we use a larger number of pictures than strictly required for the problem to be mathematically solvable. This issue is discussed in Section 3.

Nevertheless, the features of PS suggest various potential benefits for rock art, e.g., the possibility to document any site in full 3D and color by a simple commercial camera, a tripod, and a hand-positioned flash, even under direct sunlight and in restricted locations (Mannu, 2014). Not less important, the cost of the instrumentation allows for simultaneous operation on different figures by a team of researchers, without technical training.

Moreover, PS can be a highly effective tool in other situations. For instance, the volumetric reconstruction of a complex site could be managed by multi-view methods (Dyer, 2001; Slabaugh et al., 2001), leaving PS for details. Color analysis and enhancement are also important, e.g., for mixed engraved and painted sites. Here PS can provide the unique possibility to operate on the pure albedo, completely removing the shading.

Among the most recent image processing techniques applied in Archaeology, it is important to mention the ones based on polynomial texture mapping coupled to reflectance transformation imaging (PTM/RTI methods) introduced in Malzbender (2001). Some applications to rock art and to other fields of Archaeology are discussed in Duffy (2013), Earl et al. (2010) and Mudge et al. (2006). We also mention a recent study of PS with punctiform light sources, involving the solution of a system of quasi-linear partial differential equations (Mecca et al., 2014).

This paper offers a contribution to the development of effective PS techniques, and illustrates some of its improvements. In particular, computing time is reduced to minutes at full resolution, without compromising the accuracy of the computation, with the intent of making it possible to process field data in near real-time, directly on site. Moreover, the systematic use of redundant data sets by a least squares approach, coupled to a specific post processing procedure (Dessi, 2014), leads to removal or reduction of distortions. Finally, the use of a suitable computational scheme for the final integration process produces an approximation error which decreases proportionally to the square of the physical size of a pixel. Our future intent is to reach complete hands-free lighting operation, with the possibility to perform real-time 3D processing on site. Our main experimental environment consists of the decorations in the *Domus de Janas*, Neolithic tombs typical of Sardinia, Italy.

The paper is organized as follows. Section 2 describes our work from the point of view of the Archaeologist, i.e., the relevance of the tombs, their peculiarities, the challenges posed by their location, and the difficulty in restoring the details of their decorations. Section 3 introduces the mathematical setting, accounting for the computational techniques that led to a substantial improvement in the performance of PS. Practical photographic issues are addressed in Section 4, while results obtained by processing both synthetic and real data sets are illustrated in Section 5. Finally, Section 6 discusses future developments of our research.

2. Sardinia Domus de Janas

Domus de Janas are prehistoric tombs, diffused in the whole Mediterranean area, dating back to the Neolithic up to the Bronze age. In Sardinia (Italy) they assume that fascinating name that means “fairy-houses”, because of their similarity to habitations on

a smaller scale. They have been studied scientifically since the second half of the last century (Lilliu, 1967).

The past few decades have seen a growing interest on palaeoethnologic studies, focused on 212 Domus characterized by engraved, sculptured and, in few cases, painted decorations.

At the same time, digital 3D imaging technology has gained increasing relevance for Archaeology, leading to various attempt to apply such techniques to the mapping of Sardinia prehistoric tombs. This was the prompt for a critical re-consideration of the previous studies, looking for a wider perspective of the whole set of the available material, with reference to the cultural frames of the mid-western Mediterranean area. In the specific case of Sardinia Domus de Janas, the basic strategy deals with four different scopes:

- The Domus de Janas themselves, in their structural, functional, architectural, environmental, decorative, cult-related aspects, and in the outfit materials possibly found.
- The surrounding anthropic landscape, with the archaeological sources contemporary to the necropolis and, in particular, the inhabited places.
- The reconstruction of the society of the IV–III millennia B.C., with its articulation of lifestyle and economy.
- The sign function of the hypogeal art, with a deeper semeiologic and anthropologic analysis of the meaning of the signs, in order to achieve their decoding and understanding.

Within this framework, we started to develop a 3D methodology with the aim of constructing a tool for the survey of engravings and bas-reliefs, that combines a sufficient accuracy in the reconstructions, as well as the capability to deal with high resolution images by real-time computations, to ease of use. The end target is to propose an innovative way for individuating, verifying, and witnessing engraved figurative themes.

This approach has been particularly useful for developing a method of technological characterization specifically designed to catalogue the art motifs found in the necropolis named “Sos Furrighesos” in Anela (Sardinia). Our procedure fulfilled the requirement of considering engravings as cultural data in full, i. e., as elements of a concrete and specific physiognomy, that can be precisely and certainly defined because of their characteristics and peculiar traits (Tanda, 1984, p. 15–21). Such a method sets itself against the exclusively typological characterization, which uses subjective parameters, thus reaching a subjective description and interpretation.

Part of our current on-site activity consists of documenting 52 Domus de Janas. The technological characterization, followed by a typological analysis, is expected to lead to an objective interpretation of the findings, and to a contribution in the reconstruction of the operational chain of engraving arts in the hypogeal sites. In particular, the new studies should help in identifying the engraving tools and clarifying some open questions, such as the preparation of the walls, the allocation of figures in space depending on their relevance and emphasis, the partial reuse of existing figures, and the execution of superimposed schemes.

3. The computational procedure

In this section we describe the data processing stage, that is, how to pass from a set of images of an observed object, to its 3D reconstruction.

Let us assume that q digital images are available, each obtained setting the light source in a different direction ℓ_j , $j = 1, 2, \dots, q$. As it is customary, we order the pixels of each image lexicographically, i.

e., stacking the columns of the matrix containing the image into a single vector. We denote these vectors by $\mathbf{m}_1, \mathbf{m}_2, \dots, \mathbf{m}_q$; if each image is of size $r \times s$, then $\mathbf{m}_i \in \mathbb{R}^p$, with $p=rs$.

If the surface of the object is *Lambertian* (Klette et al., 1998), then the i th pixel of the j th image satisfies the relation

$$\rho_i \mathbf{n}_i^T \ell_j = m_{ij}, \quad i = 1, \dots, p, \quad j = 1, \dots, q, \quad (3.1)$$

where the scalar ρ_i is the *albedo* of the pixel, which keeps into account the partial light absorption of that portion of the surface, and which is constant for a *Lambertian reflector*. The vector \mathbf{n}_i^T is the transpose of the normal vector to the surface at that point, and m_{ij} is the radiation reflected by the i th pixel when illuminated from the direction ℓ_j . This physical law expresses the fact that the radiation reflected by the surface is proportional to the angle between the light direction and the normal to the surface (Lambert's cosine law). It can be written in matrix form as

$$RN^T L = M,$$

by grouping all the vectors in matrices as follows:

$$R = \text{diag}(\rho_1, \dots, \rho_p) \in \mathbb{R}^p \times p, \quad N = [\mathbf{n}_1, \dots, \mathbf{n}_p] \in \mathbb{R}^{3 \times p},$$

$$L = [\ell_1, \dots, \ell_q] \in \mathbb{R}^{3 \times q}, \quad M = [\mathbf{m}_1, \dots, \mathbf{m}_q] \in \mathbb{R}^{p \times q}.$$

When the lights positions are known, the matrices R and N defining the albedo and the normal vectors can be obtained by first computing

$$\tilde{N}^T = ML^\dagger,$$

where L^\dagger is the Moore–Penrose pseudoinverse of L (Björck, 1996). Then, the factorization $RN^T = \tilde{N}^T$ follows by simply normalizing the columns of \tilde{N} .

The problem with unknown lights positions (Basri and Jacobs, 2007; Chen and Chen, 2006) is much more involved. Let the compact singular value decomposition (SVD) (Golub and van Loan, 1996) of the observations matrix be

$$M = U \Sigma V^T,$$

where $\Sigma = \text{diag}(\sigma_1, \sigma_2, \sigma_3)$ is the diagonal matrix containing the singular values and $U \in \mathbb{R}^{p \times 3}$, $V \in \mathbb{R}^{q \times 3}$ are matrices whose orthonormal columns are the left and right singular vectors, respectively. This factorization can be computed efficiently by standard numerical libraries even for a large p , as the number of observed images is generally rather small ($q = 4 \sim 8$). If the data is affected by noise, this factorization may have numerical rank $k > 3$, because of error propagation. In this case, the representation may be truncated letting $\sigma_i = 0$ for $i = 4, \dots, k$.

In order to construct a rank-3 factorization of M , this matrix must obviously possess at least 3 linearly independent columns, that is, $q \geq 3$. Using a larger number of digital images of the object to be reconstructed implies a redundancy of information that may improve the results produced by the first part of the algorithm. In our experiments, we always use at least 4 input images and, when possible, we try to take up to 8 pictures, in different lighting conditions. In fact, truncation of the SVD described above produces the best rank-3 approximation to the data matrix M with respect to the Euclidean matrix norm, and the subsequent computation of the pseudoinverse matrix L^\dagger involves the solution of a least-squares problem (Björck, 1996). Both these mathematical operations have the effect to smooth the propagation of experimental noise, and to reduce the distortion of the normals due to the partial lack of Lambertianity in real rock surfaces. This may cause the occasional presence of outliers in the data set, that is, of isolated pixels in single images with a totally wrong intensity value, caused, e.g., by local specular light reflection.

If the lights ℓ_j are regularly disposed around the camera, so that their projections on the observation plane enclose equal angles,

and the slope of the light directions is kept constant, numerical evidence shows that the choice $\tilde{N} = \Sigma U^T$ and $\tilde{L} = V^T$ gives a very good approximation of the exact solution, up to normalization constants and change of signs in the rows of \tilde{N} and \tilde{L} . As a partial justification for this observation, it can be easily proved that in the presence of a regular disposition of the lights, the matrix L has orthogonal rows. The same property holds trivially for the approximate solution produced by the SVD.

We still do not have full formal proof of the above approximation property. However, our preliminary results are encouraging and suggest that a slightly modified approach could lead to the solution of the photometric stereo problem under unknown lighting in the general case, that is, without any constraints on the lights position. This situation is of great interest during field work, for the impossibility to position the lights optimally in particular archeological sites. We hope to be able to describe the algorithm, as well as an effective shooting technique, in a forthcoming paper.

Once the field of the normal vectors to the surface is known, the 3D approximation of the object, which we represent as an explicit function of two variables $z = u(x, y)$, can be recovered by solving the Poisson partial differential equation

$$\Delta u(x, y) = f(x, y),$$

where $\Delta u = u_{xx} + u_{yy}$ denotes the Laplace operator. After imposing homogenous boundary conditions on the solution, which corresponds to assuming that the observed object stands on a black background, the Poisson equation is discretized by a second order finite differences scheme. To approximate the right hand side $f(x, y)$, we differentiate numerically the x and y components of the normal vector field. We employ a central difference approximation for this computation, in order to obtain an approximation error of the same order of the integration scheme, that is, $O(h^2)$. Here h is the integration stepsize, which equals the physical size of a pixel. The value of h is not necessarily known in advance, and introduces a proportionality constant in the model, which can be chosen at will or estimated by including a ruler in one of the pictures.

The resulting square linear system of size p (number of pixels) is solved by the conjugate gradient iterative method, accelerated by an incomplete Cholesky preconditioner (Golub and van Loan, 1996). This requires a change of sign in the two sides of the system since, as it is well known, the above discretization produces a matrix which is negative definite. The total computation time for processing 4 input images on an Intel Core i5 notebook computer with 8 Gb RAM is less than 30 seconds for 1424×2144 resolution, and about 2 min for 2848×4288 resolution. Extensive numerical experiments as well as a more detailed description are reported in Dessi (2014).

In the current version of our software, written in the Matlab programming language, the computation of the solution still requires the intervention of an expert operator, who must interactively choose some parameters of the algorithm in order to produce a good 3D reconstruction. We are currently working on a version of the algorithm which is totally independent of human operation.

The mathematical model (3.1) assumes that the lights are positioned at an infinite distance from the object. In practice this constraint cannot be met, because camera flashes behave as punctiform sources. In many sites it is possible to set the light source sufficiently far away from the observed object to approximate this ideal situation, but some excavations are so narrow to make such an approach impossible. This lack of ideality leads to strong errors in low spatial frequencies of the surface, which manifests itself as a spherical distortion in 3D reconstructions. To resolve this issue, we have developed a particular post processing process that is able to stretch the surface of the object, applying

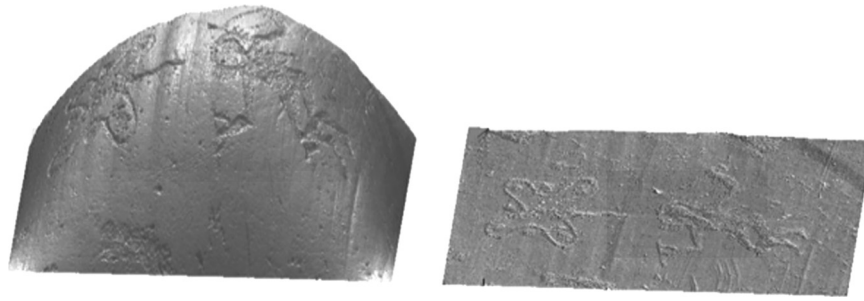


Fig. 1. The picture on the left is the 3D reconstruction (without albedo), produced by our basic algorithm, of a bas-relief found in Valcamonica, Italy (rock 24, Nature and Rock Art Reserve of Ceto, Cimbergo, and Paspardo). It represents a flower (*rosa camuna*) and an antropomorphic figure. The bowing is caused by incorrectly placed flash lights. The picture on the right is obtained by subtracting from the first image its principal component.

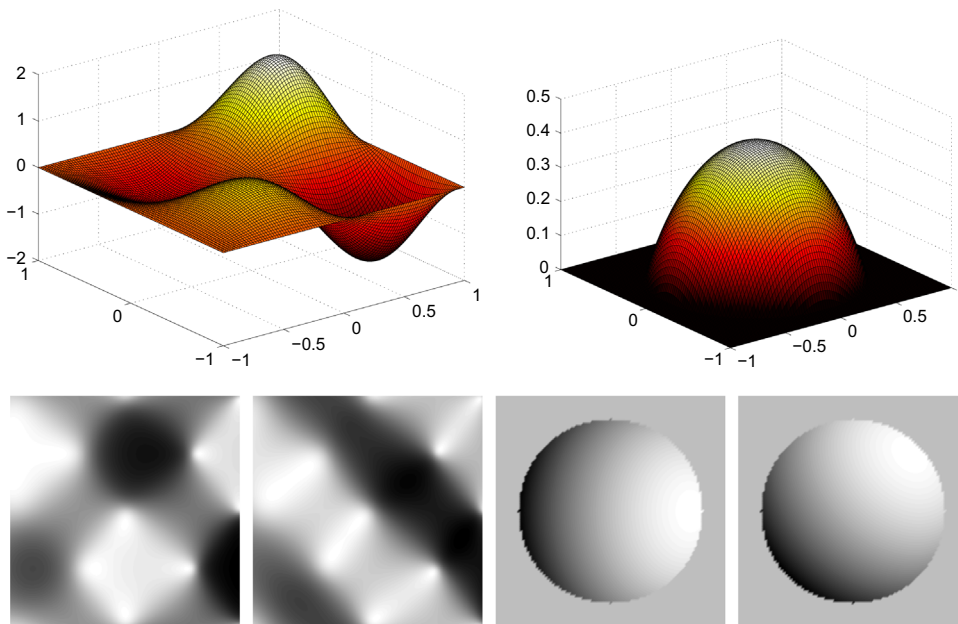


Fig. 2. The top graphs represent two synthetic objects used to investigate the performance of the algorithm described in the paper. The bottom row displays, for each object, two images produced by a direct mathematical model for PS, corresponding to different lighting conditions.

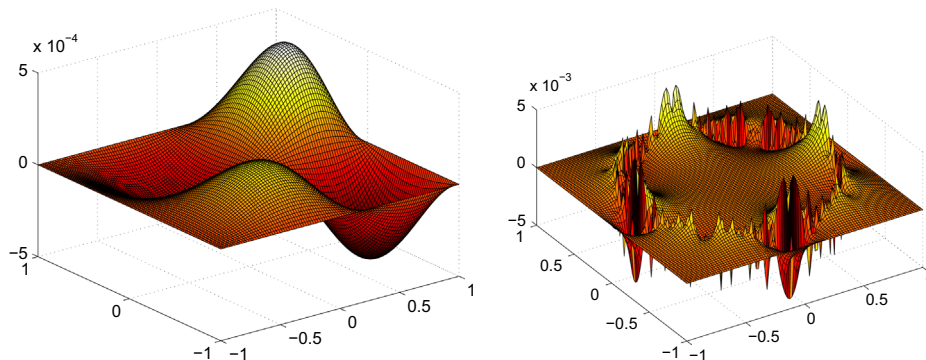


Fig. 3. The two graphs shows the pointwise error resulting from the application of our algorithm to the 3D reconstruction of the synthetic objects represented in Fig. 2. The global relative error for the two surfaces is $2.7 \cdot 10^{-4}$ and $5.0 \cdot 10^{-3}$.

standard techniques in Principal Component Analysis (Elden, 2007). It can be used only when the observed surface is approximately flat, because it tends to eliminate any curvature from the reconstruction.

Let us assume that the discretized reconstructed surface is stored in a matrix Z . We compute the first singular value γ_1 of Z , as well as the corresponding left and right singular vectors \mathbf{u}_1 and \mathbf{v}_1 .

When the size of Z is very large, this computation can be executed without actually computing the full singular system of the matrix, e.g., by the augmented implicitly restarted Golub–Kahan bidiagonalization method (Baglama and Reichel, 2005).

The so-called *principal component* of the data set is the rank one matrix $\gamma_1 \mathbf{u}_1 \mathbf{v}_1^T$. In most applicative situations, it encodes the lowest frequency component of the data. Since the bowing of the object



Fig. 4. Alghero (Sardinia), Santu Pedru necropolis, tomb of the Tetrapod Jars: double protomes overlying the entrance to a secondary cell (Contu, 1964; Tanda, 2008).

caused by the non-ideal lighting is perceived as a low frequency, compared with the carvings present on the stone, substituting the matrix Z by the difference $Z - \gamma_1 \mathbf{u}_1 \mathbf{v}_1^T$ has the effect of flattening the surface of the reconstruction. An example of the effect of this procedure is depicted in Fig. 1.

We believe that this procedure would be particularly useful to develop an automated method for “sign-extraction”, that is, a way for transforming 3D reconstruction into 2D black/white drawings, to fulfill the current standard requirement for rock art documentation. In this case, the curvature of the real surfaces should be flattened first, and then engravings and reliefs should be detected without intervention from the researcher.

4. Photographic issues

In this section we deal with technical issues concerning the application of PS to real cases. They involve cameras, lights and computer screens.

4.1. Cameras

In principle, any camera is suitable for PS. The first requirement is the possibility to switch-off automatic exposure (Mannu, 2014). The reason is clearly the need to preserve relative intensity values for each pixel when changing the light direction.

Particular care must be paid to a suitable exposure, that keeps the full dynamics of contrast within the linear region of the brightness-contrast S-shaped curve. For practical application, it is sufficient to calibrate the exposure in order to keep the three RGB histograms within the extreme boundaries of the range, avoiding that their tails reach either the total black or the total white.

In some cases, e.g., if the exposure proves to be inaccurate, it may be possible to retrieve most of the information by restricting the surface reconstruction to only one of the RGB channels. It appears, indeed, that even in moderately over-exposed pictures the blue channel is usually non-saturated, because of its lower sensitivity if compared to red and green.

Camera corrections should be computed to compensate for distortion introduced by extreme objective lenses, as wide angle or fish-eye optics. Such lenses are sometimes required by the physical conformation of the site. This is a common situation, for instance, in hypogeal tombs. However, the fixed position of the camera allows for a single correction for the whole set of images, and the correction is mandatory only when precise metrical data are required.

In particular situations, or in the presence of shooting errors, additional corrections may be required, by means of image

processing software. However, in our experience, a careful camera setting generally produces images that can be numerically processed immediately.

4.2. Lights

Depending on the subject, different lights can be chosen. When the rock decoration is under direct sunlight, the best solution is to use an electronic flash unit, with a manual setting of the camera that deeply under-exposes the picture with respect to the natural light.

Deep darkness is of course ideal for photography under artificial light. In this case even quite weak light sources can be employed. This is the case in delicate finds, such as in painted and sculptured caves. Sometimes, the flash light may be too strong, especially when the conformation of the site forces the operator to keep it close to the subject. If no other source is available, it may be advisable to process only one RGB channel of the image, as discussed in Section 4.1.

PS requires the assumption of uniform illumination and parallel light rays. This ideal condition is rather well achieved when light sources can be set at a proper distance from the framed subject, in order to cast the central part of the light beam onto the region of interest. To deal with those sites where a proper light positioning is impossible, we developed the post-processing technique discussed at the end of Section 3.

4.3. Computer screens

A very practical issue is the observation of a camera or computer display under direct sunlight. The poor performances of many LCD screens under strong external illumination conflict with the possibility, offered by PS, to have a quick check of the processed images on site, few seconds after their acquisition. The increasing diffusion of commercial sunlight-readable screens may greatly ease practical application of PS.

5. 3D reconstructions

To verify the performance of the algorithm described in Section 3 we executed an extensive set of numerical experiments, both on synthetic and field data. We report here a selection of the results. All computation were performed in double precision arithmetic using Matlab R2013a. At the moment, our software package requires some interactive intervention from an expert operator. We plan to release the software publicly, when it will be usable by non-expert users.



Fig. 5. Chermule (Sardinia), Moseddu necropolis, tomb of the Quarry: anthropomorphic figures (Contu, 1965).



Fig. 6. Ossi (Sardinia), Mesu'e Montes necropolis, tomb II: spirals on the front wall of the main cell (top), and zig-zag motifs on the right column of the main cell (bottom) (Demartis and Canalis, 1985).

To assess the accuracy attainable in the ideal situation when all the assumptions of the methods are met, we developed a direct mathematical model of PS, that allows one to choose the shape of the observed object, whose elevation is represented by an explicit mathematical function of two variables $z(x,y)$, as well as the number and direction of light sources, placed at an infinite distance from the target. From this information, the model produces the images of the object illuminated from the chosen light sources, according to Lambert's law, which can be used as input of our algorithm.

Fig. 2 shows the graphs of two objects; for each one we report two of the images generated by the model. One object is smooth, and one exhibits a discontinuity in the first partial derivatives, along a circular boundary. The resolution is fixed at 100×100 pixels, with eight light sources placed at regular angles around the object, with a 45° inclination.

We do not display the 3D reconstructions that we obtained, as they are virtually indistinguishable from the original objects. Fig. 3 shows instead, for each reconstruction, the graph of the error surface $z(x,y) - u(x,y)$, where $u(x,y)$ is the approximation produced by our algorithm. The error for the smooth object has roughly the same shape of the solution, with a much smaller scale, showing that the pointwise relative error is approximately constant. For the second object, most of the error is concentrated along the discontinuity in the first derivative of the surface, as expected, but it is only one order of magnitude larger than the previous case.

The global relative error with respect to the 2-norm, that is, the ratio $\|z - u\| / \|z\|$, is $2.7 \cdot 10^{-4}$ for the first object, $5.0 \cdot 10^{-3}$ for the second one. We observed that if the number of pixels raises, the error decreases proportionally to h^2 , being h the physical size of a pixel. This is foreseen by the error formula for the finite difference approximation used to solve the Poisson equation, and

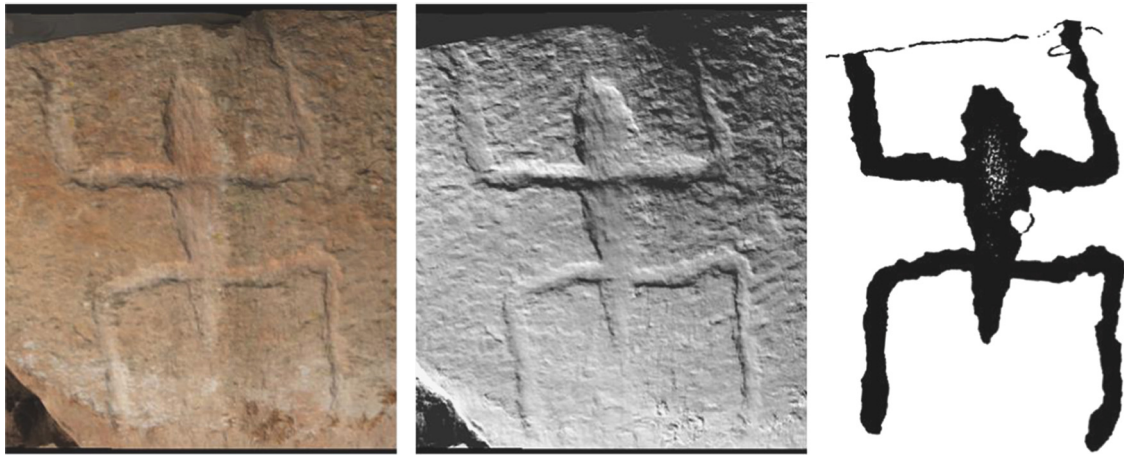


Fig. 7. Anthropomorphic figure at the necropolis of Anela: “l’orante” (the praying man) (Tanda, 1984, 2000a). 3D reconstruction with (left) or without (middle) albedo should be compared with the drawing on the right, that follows the current protocol for documenting engravings.

is in accordance with the observation that the error in the approximation of the normals is much smaller than the final error.

During the past year we have been using in our field work, which includes the survey of several Domus de Janas in Sardinia, a prototype software which implements the algorithm described in this paper. Fig. 4 shows the reconstruction of part of a tomb in the Santu Pardu necropolis, near Alghero. The picture on the left is one of the images used as input for the reconstruction, the one on the right is a snapshot of the 3D model produced by our software, that is, a completely virtual image. It is displayed after removing the albedo, with a grazing virtual lighting, in order to enhance a bas-relief whose shape is difficult to spot in the photograph. Needless to say that the observer can rotate the object and change the light direction at will, without repeating the computation. Figs. 5 and 6 display more examples of details which are almost invisible in the original pictures, but can be neatly visualized in the digital representation.

Fig. 7 shows the 3D reconstruction of a figure found in the necropolis of Anela (see Section 2). The three images report the reconstructions with and without albedo, together with a free-hand drawing which is the current standard for representation of rock art (Tanda, 2000b). The colored image is so realistic that it can be easily mistaken for a picture taken on site, rather than a computer generated reconstruction. The 3D representation (see the 3D model `anela.ply` attached to this paper) allows one to appreciate its volumetric and chromatic features. It is interesting to observe that the 3D model recovered one important feature completely lost in the drawing: the evident superposition of the arms, as a U-shaped line, onto the main body, probably executed first. This is an important remark, for the sake of the objectivity invoked in Section 2.

6. Conclusions

In this paper we propose an improved photometric stereo method as a 3D technique particularly suitable for rock art applications. Improvements are specifically related to acquisition and computing, with the result that the former now operates under free-hand lighting conditions, and the latter substantially reduces the total processing time.

In particular, the algorithm preserves all the classical advantages of PS, e.g., ease of use and requirement for relatively cheap equipment, featuring speed of computation, even for high resolution images, and sufficient accuracy for documentation purposes.

The problem of surface distortion, caused by punctiform lights, is partially solved by a numerical procedure.

The non-ideality of real light sources is a problem that still calls for a deeper analysis, as well as the possibility to extract information on the positioning of lights directly from the data set. A deep comprehension of this issues, with special attention to the extraction of accurate metric information from the reconstructions, would allow for the introduction of a standard protocol for storing and sharing documental data in Archaeology, with the possibility of making available a much larger amount of information by digital 3D methods, compared to traditional approaches.

Appendix A. Supplementary data

Supplementary data associated with this paper can be found in the online version at <http://dx.doi.org/10.1016/j.daach.2015.05.002>.

References

- Baglama, J., Reichel, L., 2005. Augmented implicitly restarted Lanczos bidiagonalization methods. *SIAM J. Sci. Comput.* 27, 19–42.
- Barsky, S., Petrou, M., 2003. The 4-source photometric stereo technique for three-dimensional surfaces in the presence of highlights and shadows. *IEEE Trans. Pattern Anal. Mach. Intell.* 25 (10), 1239–1252.
- Basri, R., Jacobs, D.J., Kemelmacher, I., 2007. Photometric stereo with general, unknown lighting. *Int. J. Comput. Vis.* 72 (3), 239–257.
- Björck, Å., 1996. Numerical Methods for Least Squares Problems. SIAM, Philadelphia.
- Chen, C.P., Chen, C.S., 2006. The 4-source photometric stereo under general unknown lighting. In: *Computer Vision-ECCV, 2006*, Springer, Vienna, pp. 72–83.
- Christensen, P.H., Shapiro, L.G., 1994. Three-dimensional shape from color photometric stereo. *Int. J. Comput. Vis.* 13 (2), 213–227.
- Contu, E., 1964. La tomba dei vasi tetrapodi in loc. Santu Pedru (Alghero-Sassari). *Monumenti Antichi dell’Accademia dei Lincei*, XLVII, 1964.
- Contu, E., 1965. Nuovi petroglifi schematici della Sardegna. *Bull. Paletnol. Ital.* XVI 74, 69–122.
- Demartis, G.M., Canalis, V., 1985. La tomba Il di Mesu’e Montes (Ossi-Sassari). *Nuovo Bull. Archeol. Sardo* 2, 41–74.
- Dessì, R., 2014. Algoritmi Ottimizzati per la Photometric Stereo Applicati all’Archaeologia (Bachelor’s Thesis in Electrical and Electronics Engineering), University of Cagliari. Available at: URL (<http://bugs.unica.it/~gppe/did/tesi/14dessi>).
- Duffy, S.M., 2013. Multi-light imaging techniques for heritage application. English Heritage, Product code: 51802, English Heritage Publishing, available at: (<https://www.historicengland.org.uk/images-books/publications/multi-light-imaging-heritage-applications/>).
- Dyer, C.R., 2001. Volumetric scene reconstruction from multiple views, *Foundations of Image Understanding*. Springer, Vienna, pp. 469–489.
- Earl, G., Beale, G., Martinez, K., Pagi, H., 2010. Polynomial texture mapping and related imaging technologies for the recording analysis and presentation of

- archaeological materials. In: ISPRS Commission V Midterm Symposium, Newcastle, UK, 2010, pp. 218–223.
- Eldén, L., 2007. Matrix Methods in Data Mining and Pattern Recognition, volume 4 of Fundamentals of Algorithms. SIAM, Philadelphia, 2007.
- Golub, G.H., van Loan, C.F., 1996. *Matrix Computations*, third ed. The John Hopkins University Press, Baltimore.
- Klette, R., Schlüns, K., Koschan, A., 1998. *Computer Vision: Three-dimensional Data from Images*. Springer, Singapore.
- Lilliu, G., 1967. *Civiltà La, dei Sardi dal Neolitico all'Età dei Nuraghi* Edizioni ERI, Torino, 1967.
- Malzbender, T., Gelb, D., Wolters, H., 2001. Polynomial texture maps. In Proceedings of the 28th Annual Conference on Computer Graphics and Interactive Techniques, 2001, ACM, New York, pp. 519–528.
- Mannu, C., 2014. 3D Photometric Stereo per l'Arte Preistorica (Bachelor's Thesis in Electrical and Electronical Engineering), University of Cagliari. Available at: URL (<https://www.academia.edu/8502503/3DPhotometricStereoPerlArtePreistorica>).
- Mecca, R., Wetzler, A., Bruckstein, A.M., Kimmel, R., 2014. Near field photometric stereo with point light sources. *SIAM J. Imaging Sci.* 7, 2732–2770.
- Mudge, M., Malzbender, T., Schroer, C., Lum, M., 2006. New reflection transformation imaging methods for rock art and multiple-viewpoint display. In: VAST, vol. 6, 2006, pp. 195–202.
- Slabaugh, G., Culbertson, B., Malzbender, T., Schafer, R., 2001. A survey of methods for volumetric scene reconstruction from photographs. In: Proceedings of the 2001 Eurographics Conference on Volume Graphics, Springer, Vienna, 2001, pp. 81–100.
- Tanda, G., 1984. In: Chiarella (Ed.), *Arte e Religione della Sardegna Preistorica nella Necropoli di Sos Furrighesos-Anela*. Chiarella Editore, Sassari, 1984.
- Tanda, G., 2000. La tomba XV di Sos Furrighesos, Anela (SS). In: *Atti del Congresso Internazionale: L'Ipogeismo nel Mediterraneo: Origini, Sviluppo, Quadri Culturali*, 23–28 maggio 1994, 2000, pp. 931–933.
- Tanda, G., 2000. L'ipogeismo in sardegna: arte, simbologia, religione. In: *Atti del Congresso Internazionale: L'Ipogeismo nel Mediterraneo: Origini, Sviluppo, Quadri Culturali*, 23–28 maggio 1994, 2000, pp. 399–425.
- Tanda, G., 2008. Il segno e l'idea. le figurazioni scolpite di bucranio nella preistoria della sardegna. In: Tanda, G. Lugliè, C. (Eds.), *Il Segno e l'Idea. Arte preistorica in Sardegna*, Cagliari, 2008. CUEC.
- Woodham, R.J., 1980. Photometric method for determining surface orientation from multiple images. *Opt. Eng.* 19 (1), 191139.